

1 Linking photoacclimation responses and microbiome shifts 2 between depth-segregated sibling species of reef corals

3
4 Carlos Prada^{1*+}, Tomás López-Londoño²⁺, F. Joseph Pollock^{2,3}, Sofia Roitman², Kim B. Ritchie⁴,
5 Don R. Levitan⁵, Nancy Knowlton⁶, Cheryl Woodley⁷, Roberto Iglesias-Prieto¹, Mónica Medina¹

6 ¹University of Rhode Island, Department of Biological Sciences, Kingston, RI 02881, USA

7 ²Pennsylvania State University, Department of Biology, 208 Mueller Lab, University Park, PA 16802, USA

8 ³The Nature Conservancy, Hawai'i and Palmyra Programs, 923 Nu'uuanu Avenue, Honolulu, HI 96817, USA

9 ⁴University of South Carolina Beaufort, Department of Natural Sciences, 801 Carteret Street, Beaufort, SC
10 29906, USA

11 ⁵Florida State University, Department of Biological Science, Tallahassee, FL 32306, USA

12 ⁶National Museum of Natural History, Smithsonian Institution, Washington, DC 20560, USA

13 ⁷National Oceanic and Atmospheric Administration, National Ocean Service, National Centers for Coastal
14 Ocean Sciences, Hollings Marine Laboratory, Charleston, SC 29412, USA.

15 *Corresponding author: prada@uri.edu.

16 +Equal contribution.

18 ABSTRACT

19 Metazoans host complex communities of microorganisms that include dinoflagellates, fungi, bacteria,
20 archaea, and viruses. Interactions among members of these complex assemblages allow hosts to adjust
21 their physiology and metabolism to cope with environmental variation and occupy different habitats.
22 Here, using reciprocal transplantation across depths, we studied adaptive divergence in the Caribbean
23 corals *Orbicella annularis* and *O. franksi*. When transplanted from deep to shallow, *O. franksi*
24 experienced fast photoacclimation, low mortality, and maintained a consistent bacterial community. In
25 contrast, *O. annularis* experienced higher mortality, and limited photoacclimation when transplanted
26 from shallow to deep. The photophysiological collapse of *O. annularis* in the deep environment was
27 associated with an increased microbiome variability and reduction of some bacterial taxa. Differences in
28 the symbiotic algal community were more pronounced between coral species than between depths. Our
29 study suggests that these sibling species are adapted to distinctive light environments partially driven by
30 the algae photoacclimation capacity and the microbiome robustness, highlighting the importance of
31 niche specialization in symbiotic corals for the maintenance of species diversity. Our findings have
32 implications for the management of these threatened Caribbean corals and the effectiveness of coral
33 reef restoration efforts.

34 **Keywords:** corals, symbiosis, microbiome, photobiology, ecophysiology, niche divergence

35 INTRODUCTION

36 Understanding how microbial biodiversity interacts with their host's physiology is essential for
37 understanding animal ecology and evolution (Thompson et al. 2015). Microbial communities often fine-
38 tune their host's physiology to cope with environmental variation across habitats (Gilbert et al. 2010).
39 Reef-building corals (Cnidaria: Scleractinia) form a symbiotic association with dinoflagellates, which
40 allow corals to thrive on the ocean's euphotic zone along a strong depth-mediated light gradient
41 (Stoddart 1969). Corals living at different depths possess distinctive physiological and morphological
42 traits to optimize energy acquisition which results from genotypic and phenotypic variation within and
43 between coral species (Vermeij and Bak 2002; Hoogenboom et al. 2008). Coral colonies at different
44 depths may host distinctive symbiotic algae with contrasting photoacclimation capabilities that grant
45 their hosts the ability to thrive in certain light environments (Rowan et al. 1997; Warner et al. 2006).
46 Because of these differences in photoacclimation and the prevalence of specific associations with coral
47 hosts, zonation by light has been regarded as a primary form of niche partitioning in symbiotic corals
48 (Iglesias-Prieto et al. 2004).

49 While the influence of different species of symbiotic algae on the ecophysiology of reef-building corals
50 has been studied, the effect of other coral-associated microorganisms is less known, specially across
51 depth-segregated species (Rohwer et al. 2002; Pantos et al. 2015). However, the interest on coral-
52 associated microbes and their roles in maintaining health and preventing diseases has increased
53 substantially (Kellogg et al. 2013; Peixoto et al. 2017). From an eco-evolutionary perspective, the
54 evidence suggests that coral-associated bacterial assemblages can be highly variable although
55 "footprints" of unique microbial assemblages appear to be mediated by a combination of host species
56 and local environmental conditions (Rohwer et al. 2002; Marchioro et al. 2020). These patterns indicate
57 that bacterial communities, like photosynthetic dinoflagellates, could also be spatially structured and
58 segregated along environmental gradients.

59 Recently diverged coral species that differ in their vertical distribution are ideal systems to study the
60 microbiota-animal relationship as a potential basis for habitat specialization. The *Orbicella* species
61 complex, dominant in Caribbean reefs, was initially regarded as one species with ecotypic variation, but
62 recent research revealed three species partially segregated by depth (Weil and Knowlton 1994; Fukami
63 et al. 2004; Levitan et al. 2011). *O. annularis* is a high-light specialist which forms columns with
64 senescent edges, while *O. franksi* is a low-light specialist forming irregular mounds and plates. *O.*

65 *faveolata* form massive mounds and can overlap with both *O. annularis* and *O. franksi* habitats. The
66 three *Orbicella* species are closely related with incomplete lineage sorting across nuclear and
67 mitochondrial markers (Weil and Knowlton 1994; Fukami et al. 2004). The symbiotic dinoflagellate
68 communities (Rowan et al. 1997; Kemp et al. 2015) as well as the photobiology of this species complex
69 have been extensively studied (Warner et al. 2006; Scheufen et al. 2017), enabling the identification of
70 important differences mediated by environmental gradients. The *Orbicella*-associated bacterial
71 communities have also been examined (Kellogg et al. 2013; Roitman et al. 2020). Therefore, this coral
72 species complex offers an ideal system for the study of how species specialize to live in different
73 habitats through adaptive divergence.

74 Using a reciprocal transplant experiment between shallow and deep environments in Bocas del Toro
75 (Caribbean Panama), we studied adaptive divergence between the youngest sister species within the
76 *Orbicella* species complex, *O. annularis* and *O. franksi*. We surveyed colonies for survivorship and
77 characterized the algal symbiont and microbial communities across habitats. We also evaluated if these
78 recently diverged species have also diverged physiologically along depth-mediated light gradients. We
79 hypothesize that *O. franksi* and *O. annularis* exploit different light niches, coexisting in Caribbean reefs
80 with minimal competition for space. Our findings suggest that despite being so young (< 500K) (Pandolfi
81 et al. 2002), these two sister species have diverged and fine-tuned their photoacclimation capabilities
82 and microbial symbionts to maximize efficiency in their own light environments.

83 MATERIALS AND METHODS

84 ***Reciprocal transplantation***

85 To study the effects of depth and light in *O. annularis* and *O. franksi*, colonies were reciprocally
86 transplanted between shallow and deep environments at Bocas del Toro, Panama (latitude: 9.327222,
87 longitude: -82.203889). The study site is located on the slope of a relative narrow reef protected on all
88 sides by islands and has been monitored for coral spawning for two decades (Levitan et al. 2011). This
89 location is ideal to study adaptation across depths because the vertical distribution of these species is
90 compressed to shallower depths (~2-9 m) compared to other sites in the Caribbean (Van Veghel 1994;
91 Pandolfi and Budd 2008), although maintaining the typical vertical zonation pattern (*O. annularis* in
92 shallow-water and *O. franksi* in deeper-water).

93 In September 2014, fully pigmented coral clonemate fragments (~5 cm in diameter) were collected from
94 the edges of *O. franksi* colonies and vertically oriented colonies of *O. annularis*. Same genotypes
95 (clonemates) of both species ($n \leq 28$) were exposed to both shallow and deep environments. Coral
96 fragments were collected from two depths in which each species was abundant: shallow for *O. annularis*
97 (3–4 m) and deep for *O. franksi* (7–8 m). Coral fragments from each species were transplanted to
98 polyvinyl chloride (PVC) panels placed near the original depth of collection (3.5 m and 9.5) where they
99 were left to heal and acclimate for one week. Subsequently, *O. annularis* colonies were transplanted
100 from shallow to shallow (S-S) ($n = 27$) and shallow to deep (S-D) ($n = 30$). Similarly, *O. franksi* colonies
101 were transplanted from deep to shallow (D-S) ($n = 44$) and deep to deep (D-D) ($n = 28$).

102 To test for differential mortality across depths, we visually inspected colonies six months after
103 transplantation in March 2015. One detached individual from *O. annularis* transplanted deep was
104 discarded from this analysis. A one-tailed Fisher exact test was used to assess differences in survivorship
105 among sites. To standardize the fitness (*i.e.*, survival) advantage on the original depth over the opposite
106 depth for each species, differences in fitness were divided over the average fitness on each particular
107 habitat (Hereford 2009).

108 Samples were collected in accordance with local regulations under CITES permits PWS2014-AU-002155
109 and 12US784243/9 and Panama permit number SE/A-94-13.

110 ***Environmental parameters***

111 To characterize the effect of the water optical properties on light availability across depths, we
112 measured the diffuse attenuation coefficient for downwelling irradiance (K_d) at the beginning of the
113 experiment. K_d was calculated by measuring changes in light intensities across the depth gradient using
114 the cosine-corrected PAR sensor of a Diving-PAM (Walz), previously calibrated against a manufacturer-
115 calibrated quantum sensor (LI-1400, LI-COR). The light intensity at each transplant site, expressed as the
116 percentage of incident light, was calculated (Kirk 2011; López-Londoño et al. 2021). Variation in
117 temperature and relative light levels throughout the duration of the experiment was recorded every 30
118 min by Onset HOBO data loggers (UA-002-64, Onset Computer Corporation) attached to the PVC panels.

119

120

121 **Photophysiology**

122 To test how depth-dependent light variation affects the photosynthetic condition of corals' symbiotic
123 algae, we measured the chlorophyll *a* (Chl *a*) fluorescence using pulse amplitude modulated (PAM)
124 fluorometry (Diving-PAM). Measurements were recorded on ten fragments from each species at each
125 depth before transplantation, and every two/three days during the week after transplantation. The
126 effective quantum yield ($\Delta F/F_m'$) of photosystem II (PSII) was recorded at noon during peak sunlight
127 exposure, and the maximum quantum yield of PSII (F_v/F_m) at dusk. The maximum excitation pressure
128 over PS II (Q_m) was calculated as $Q_m = 1 - [(\Delta F/F_m')/(F_v/F_m)]$ (Iglesias-Prieto et al. 2004). $\Delta F/F_m'$ was also
129 recorded *in situ* on coral colonies of *O. annularis* ($n = 38$) and *O. franksi* ($n = 67$) randomly distributed
130 over the full depth range of each species. In order to calculate Q_m on these colonies, we estimated F_v/F_m
131 based on a linear regression with data obtained from a sub-sample of colonies randomly distributed
132 over the same depth range ($n = 10$ and $n = 21$ for *O. annularis* and *O. franksi*, respectively). Pearson's
133 correlation coefficients revealed a strong positive correlation between F_v/F_m and depth in both *O.*
134 *annularis* and *O. franksi* ($R^2 = 0.85$, $p < 0.01$ and $R^2 = 0.83$, $p < 0.01$), indicating a reliable prediction of
135 F_v/F_m across depths. We used linear regression models to explore the relationship between Q_m and
136 depth for *O. annularis* and *O. franksi* based on evidence that Q_m varies in a pattern that is roughly linear
137 with depth in other coral species (Iglesias-Prieto et al. 2004). An Analysis of Covariance (ANCOVA) was
138 conducted to test for differences in slopes and intercepts among regression models (interaction of
139 species with depth). Due to technical issues with the Diving-PAM (loss in hermeticity), samples from the
140 transplant experiment were transported from the transplant sites to the boat in a dark container to
141 record measurements. During this short period of dark acclimation (<5 min), some components of the
142 non-photochemical quenching could have relaxed (Ralph and Gademann 2005), leading to a slight, yet
143 nearly constant, underestimation of the $\Delta F/F_m'$ recorded at noon and, as a result, of Q_m in all corals.
144 Analyses were conducted using R version 3.6.1 (R Core Team 2015).

145 **Microbiome**

146 *Small Subunit Ribosomal RNA (16S) amplicon library preparation and sequencing, sequence quality*
147 *control and initial data processing*

148 We quantified coral-associated microbiome communities in coral transplants to test if adaptive
149 divergence between *O. annularis* and *O. franksi* is in part due to their microbial communities. Tissue

150 samples were collected at the end of the transplant experiment using 1/8" metal corers by divers
151 wearing Nitrile gloves and were immediately deposited in whirl pack bags. Once returned to the boat,
152 each sample was gently washed with filter-sterile (0.2 μm) seawater, deposited in a sterile cryovial, and
153 immediately preserved in liquid nitrogen. We extracted DNA from coral tissue samples using the MoBio
154 Powersoil DNA Isolation Kit (MoBio Laboratories). Two-stage amplicon PCR was performed on the V4
155 region of the 16S small subunit prokaryotic rRNA gene (Apprill et al. 2015; Roitman et al. 2020). First, 30
156 PCR cycles were performed using 515F and 806R primers (underlined) with linker sequences at the 5'
157 ends: 515F_link (5'-ACA CTG ACG ACA TGG TTC TAC AGT GCC AGC MGC CGC GGT AA-3') and 806Rb_link
158 (5'-TAC GGT AGC AGA GAC TTG GTC TGG ACT ACH VGG GTW TCT AAT-3'). Each 20 μL PCR reaction was
159 prepared with 9 μL 5Prime HotMaster Mix (VWR International), 1 μL forward primer (10 μM), 1 μL
160 reverse primer (10 μM), 1 μL template DNA (~20 ng/ μL), and 8 μL PCR-grade water. PCR amplifications
161 consisted of a 3 min denaturation at 94 $^{\circ}\text{C}$; 30 cycles of 45 s at 94 $^{\circ}\text{C}$, 60 s at 50 $^{\circ}\text{C}$ and 90 s at 72 $^{\circ}\text{C}$; and
162 10 min at 72 $^{\circ}\text{C}$. Amplicons were barcoded with Fluidigm barcoded Illumina primers (8 cycles) and
163 pooled in equal concentrations for sequencing. The amplicon pool was purified with AMPure XP beads
164 and sequenced on the Illumina MiSeq sequencing platform at the DNA Services Facility at the University
165 of Illinois at Chicago. Sequences were submitted to the National Center for Biotechnology Information
166 (NCBI) Short Read Archive (SRA) under project number PRJNA717688.

167 Initial processing of 16S libraries was performed using the Quantitative Insights Into Microbial Ecology
168 (QIIME; v1.9) package (Caporaso et al. 2010b). Primer sequences were trimmed, paired-end reads
169 merged, and QIIME's default quality-control parameters were used to split libraries among samples.
170 Chimeras were removed and 97%-similarity OTUs picked using USEARCH 7.0 (Edgar 2010), QIIME's
171 subsampled open-reference OTU-picking protocol (Rideout et al. 2014), and the 97% GreenGenes 13_8
172 reference database (McDonald et al. 2012). Taxonomy was assigned using UCLUST and reads were
173 aligned against the GreenGenes database using PyNASt (Caporaso et al. 2010a). FastTreeMP (Price et al.
174 2010) was used to create a bacterial phylogeny with constraints defined by the GreenGenes reference
175 phylogeny. OTUs classified as "unknown" (*i.e.*, sequences not classified at the kingdom level),
176 chloroplast, mitochondria, or other potential contaminants were removed. Low coverage samples (< 223
177 useable reads) were omitted. Unless otherwise stated, downstream microbiome analyses and figure
178 generation were performed in R version 3.2.5 (R Core Team 2015) using the phyloseq and ggplot2
179 packages (Wickham 2009; McMurdie and Holmes 2013).

180

181 *β-diversity group significance and differential abundance testing*

182 To quantify differences among treatments, we used weighted UniFrac (wUniFrac) dissimilarity matrices
183 using OTU-level relative abundances. Significant differences in bacterial assemblages were assessed by
184 permutational multivariate analysis of variance (PERMANOVA) with wUniFrac distances and the
185 explanatory variables host species and depth (*i.e.*, `vegan::adonis`) (Oksanen et al. 2017). Both overall
186 (*i.e.*, *O. annularis* and *O. franksi*) and species-specific models (*i.e.*, *O. annularis* or *O. franksi*) were tested.
187 Heatmaps of OTU abundances were created using the `phyloseq::plot_heatmap` function (McMurdie and
188 Holmes 2013). Within-category microbiome variability (*i.e.*, wUniFrac distance) was calculated in QIIME
189 using the `make_distance_boxplots` function, which also assesses significant differences in microbiome
190 variability among categories via pairwise, nonparametric t-tests (1000 Monte Carlo permutations) with
191 Bonferroni correction. To test for significant differences in OTU abundances across host species and
192 depths, we employed negative binomial modelling using DESeq2 (McMurdie and Holmes 2013; Love et
193 al. 2014). Both the overall (*i.e.*, *O. annularis* and *O. franksi*) and species-specific models (*i.e.*, *O. annularis*
194 or *O. franksi*) were tested. P-values for the significance of contrasts were generated based on Wald
195 statistics, and false discovery rates were calculated using the Benjamini–Hochberg procedure.

196 ***Microalgal communities***

197 *Internal Transcribed Spacer 2 rRNA (ITS2) amplicon library preparation, sequencing, and initial*
198 *processing*

199 To quantify differences in dinoflagellate communities across species and depths, we used a two-stage
200 amplicon PCR on the same DNA that was extracted and used for the 16S amplification. We amplified the
201 Internal Transcribed Spacer 2 (ITS2) rRNA marker gene commonly used for identification of
202 Symbiodiniaceae (Hume et al. 2019). The primers used to quantify differences in the symbiotic algal
203 communities were modified versions of the ITS-DINO forward (5'-ACA CTG ACG ACA TGG TTC TAC AGT
204 GAA TTG CAG AAC TCC GTG-3') and ITS2Rev2 (5'- TAC GGT AGC AGA GAC TTG GTC TCC TCC GCT TAC TTA
205 TAT GCT T-3') (Stat et al. 2009) that include the universal primer sequences required for Illumina MiSeq
206 amplicon sequencing, namely common sequence 1 (CS1) and common sequence 2 (CS2). The PCR
207 amplification was structured as follows: 2 min of denaturation at 94 °C; 35 cycles of 45 s at 94 °C, 60 s at
208 55 °C, and 90 s at 68 °C; then finally 7 min at 68 °C. Once the PCR reactions were finished, samples were
209 held at 4 °C before sequencing. Samples were sequenced using the Illumina MiniSeq platform at the
210 DNA Services Facility at the University of Chicago, Illinois. Sequences were submitted to SymPortal for

211 processing and quality checks (Hume et al. 2019). Quality checking was performed using mothur (Schloss
212 et al. 2009), followed by taxonomic identification using blastn. The SymPortal pipeline then subdivides
213 sequences into genus groupings and identified type profiles, referred to as defining intragenomic
214 sequence variants (DIVs). Type profiles were only identified if a variant contained more than 200
215 sequences, and the sequences were subsequently named based on whether they had been used in the
216 definition of the DIVs. The resulting absolute and relative count tables were imported into R version
217 3.5.2 (R Core Team 2015) for downstream analyses and figure generation using the phyloseq (McMurdie
218 and Holmes 2013), vegan (Oksanen et al. 2017), microbiome (Lahti and Shetty 2017), and ggplot2
219 (Wickham 2009) packages.

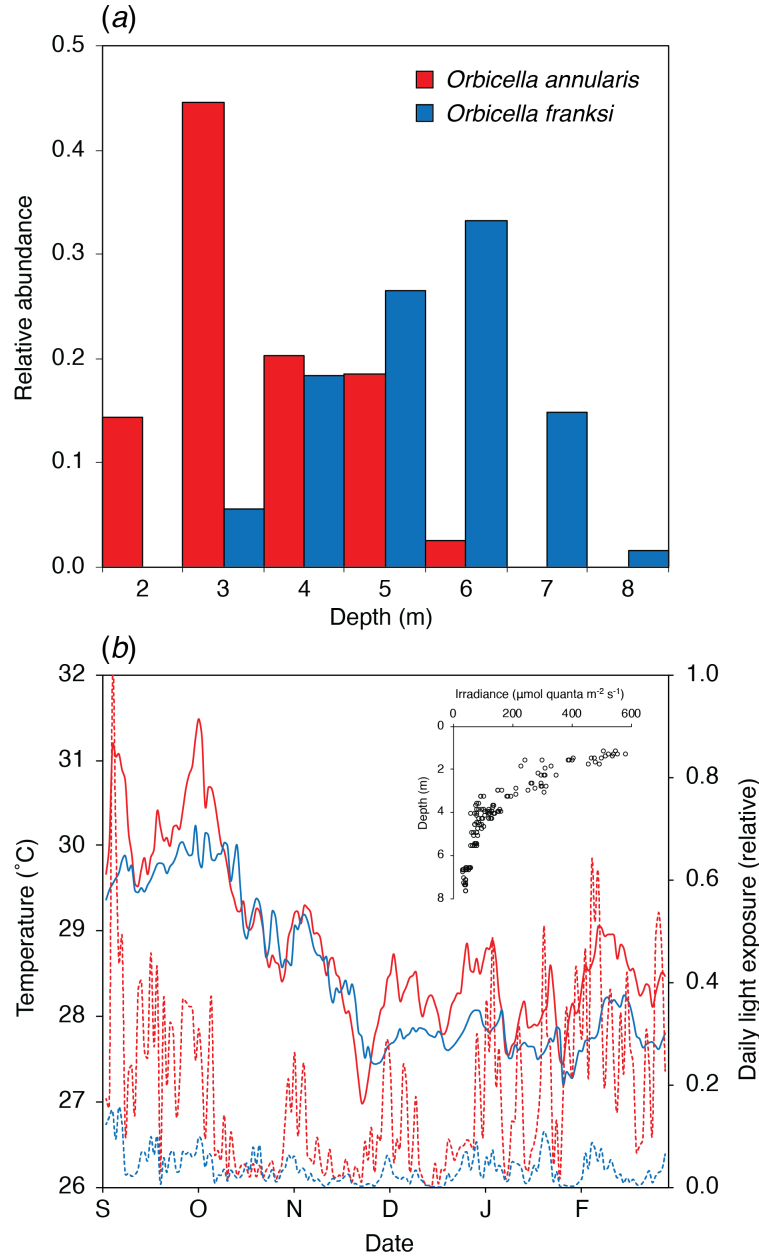
220 *β-diversity group significance testing*

221 To compare dinoflagellate communities across samples, we constructed Bray-Curtis and Jaccard
222 dissimilarity matrices using absolute abundances. Significant differences in bacterial communities
223 between sample types were assessed by PERMANOVA with Bray-Curtis and Jaccard distances and
224 explanatory variables including host species, season, and depth using the adonis function from the
225 vegan package (Oksanen et al. 2017). We tested overall models that encompassed both species as well
226 as species-specific models.

227 RESULTS

228 ***Temperature and irradiance are higher and more variable in shallow environments***

229 The K_d near the transplant sites was 0.40 m^{-1} , indicating that corals from the shallow (3.5 m) and deep
230 (9.5 m) sites receive respectively ~25% and ~2% sea surface irradiance. Across the vertical distribution
231 range of each species (**Fig 1a**), it is estimated that the light intensity varies between 18% and 62% sea
232 surface irradiance for *O. annularis* and between 5% and 33% for *O. franksi*. Relative light levels recorded
233 by data loggers indicated that the light exposure was nearly 5 times more variable in shallow water than
234 in deep water. Daily temperatures were significantly higher in the shallow site ($28.85 \pm 0.96 \text{ }^\circ\text{C}$, mean \pm
235 s.d.) than in the deep site ($28.46 \pm 0.88 \text{ }^\circ\text{C}$; t -value = 3.92, $p < 0.001$; **Fig. 1b**). However, based on the
236 scaling quotient of temperature (Q_{10}) of *Orbicella* spp. (Scheufen et al. 2017), it is estimated that the
237 metabolic rate variation due to differences in temperature among sites is negligible (~5%).



238

239 **Figure 1.** (a) Vertical distribution of *O. annularis* and *O. franksi* around the transplant sites in Bocas del
240 Toro, Panamá, previously established as part of the long-term monitoring of coral spawning (Levitan et
241 al. 2011). (b) Variation of the mean daily temperature (continuous lines) and relative light exposure
242 (discontinuous lines) at the shallow (red) and deep (blue) transplant sites. The inset shows the light
243 intensity variation across depths used to calculate the local K_d .

244

245

246

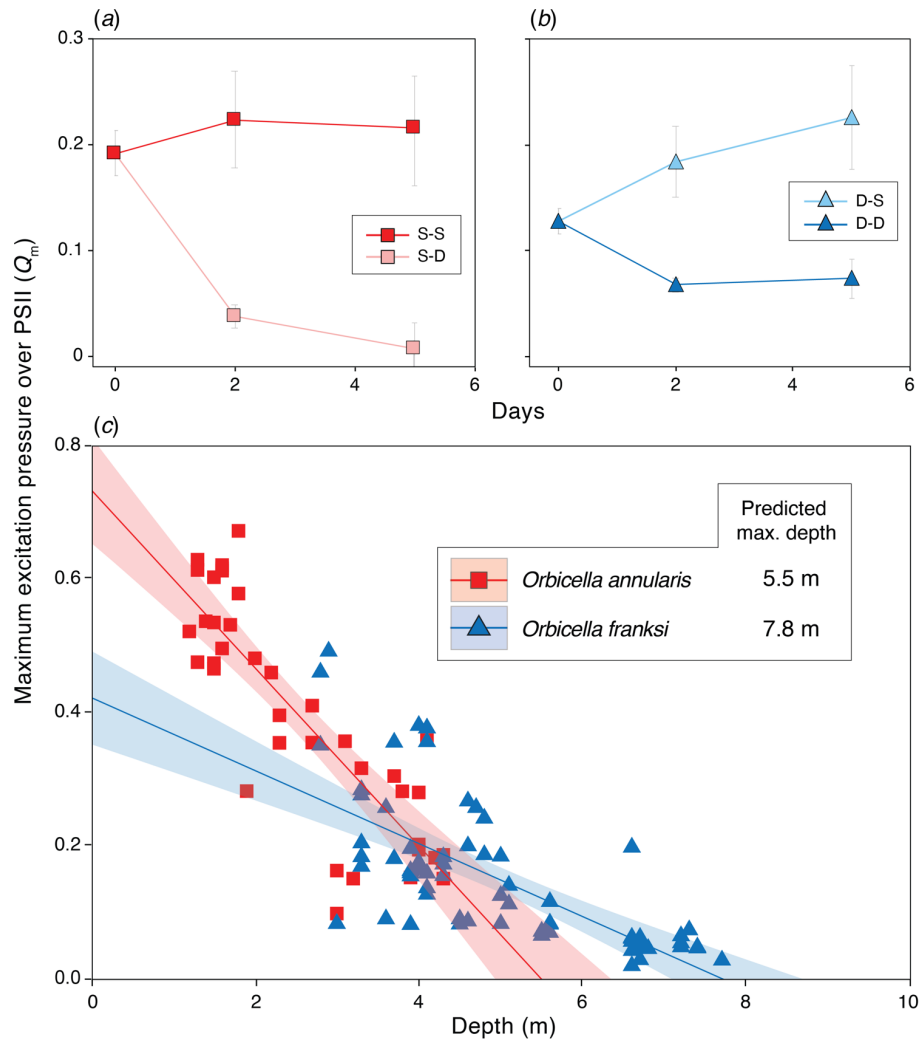
247 ***O. annularis* experiences greater mortality in deep environments**

248 Transplantation of *O. annularis* S-D ($\Delta_{\text{depth}} = 6$ m) resulted in 26% mortality (Fisher exact test: $p = 0.003$)
249 and was significantly higher than that of *O. franksi* colonies transplanted D-D (4% mortality, Fisher exact
250 test: $p = 0.04$). *O. franksi* therefore has an advantage of 26% over *O. annularis* in deep habitats. In
251 contrast, *O. franksi* when transplanted D-S did remarkably well with only 2% mortality (Fisher exact test:
252 $p = 0.63$). Mortality of the two species was not significantly different (0% mortality, Fisher exact test: $p =$
253 0.60), suggesting that *O. franksi* in shallow areas has no perceivable short-term (< six months)
254 disadvantage relative to *O. annularis* (Fisher exact test: $p = 0.60$).

255 **Photoacclimation of *O. annularis* is insufficient to compensate for reduced light**

256 Symbionts of *O. annularis* exhibited a significant increase in F_v/F_m when transplanted S-D (0.622 ± 0.034)
257 relative to corals transplanted S-S (0.541 ± 0.007) (t -value = -6.25, $p < 0.01$). On the contrary, symbionts
258 of *O. franksi* transplanted D-S experienced a reduction in F_v/F_m (0.470 ± 0.052) relative to D-D
259 transplants (0.630 ± 0.020 ; t -value = 0.55, $p < 0.01$). Transplantation of *O. annularis* S-D induced a
260 significant reduction in Q_m (0.008 ± 0.076), relative to S-S transplantation (0.216 ± 0.163 ; t -value = 3.67,
261 $p < 0.01$) (**Fig. 2a**); while *O. franksi* exhibited a significant increase in Q_m (0.226 ± 0.156) when
262 transplanted D-S, relative to D-D transplants (0.073 ± 0.056 ; t -value = 3.26, $p < 0.01$) (**Fig. 2b**).

263 Estimations of Q_m on coral colonies along the vertical distribution of each species ranged from 0.099 to
264 0.673 in *O. annularis* and from 0.020 to 0.492 in *O. franksi* (**Fig. 2c**). We found a significant species by
265 depth interaction ($F_{(1,102)}=28.78$, $p<0.001$), indicating that the slope of the regression model describing
266 the relationship between Q_m and depth was significantly different between species, being more than
267 twice as pronounced in *O. annularis* ($m=-0.13$; $R^2=0.71$, $p<0.001$) than in *O. franksi* ($m=-0.05$; $R^2=0.50$,
268 $p<0.001$). The linear regression of Q_m with depth indicated that the potential depth limit described by
269 the bioenergetics of the coral-algae symbiosis (*i.e.*, where Q_m reaches the minimum theoretical value of
270 0) is 5.5. m for *O. annularis* and 7.8 m for *O. franksi* (**Fig. 2c**), which nearly coincide with the observed
271 lower limit of distribution of both species in the study area (**Fig. 1a**).



272

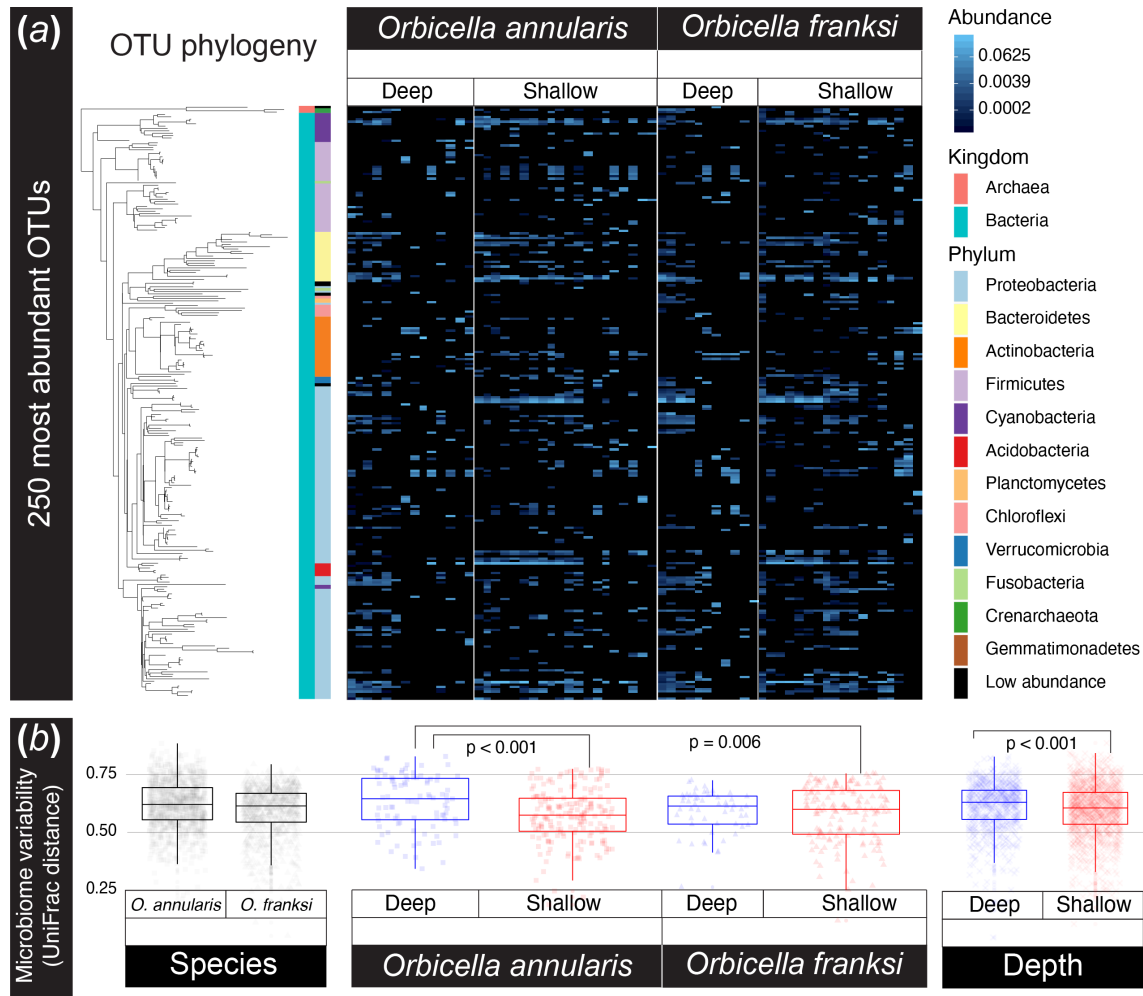
273 **Figure 2.** Photoacclimation responses of *Orbicella* spp. across depths. Maximum excitation pressure over
 274 PS II (Q_m) is shown pre- and post-transplantation for *O. annularis* (a) and *O. franksi* (b). Values obtained
 275 in *O. annularis* transplanted S-S are shown in dark red while those transplanted S-D in pink. Values from
 276 *O. franksi* transplanted D-D are shown in dark blue while those transplanted D-S in light blue. (c) Q_m
 277 variation in *O. annularis* (red) and *O. franksi* (blue) along a depth gradient. A linear model was used to fit
 278 the data and predict the maximum potential depth limit described by Q_m for *O. annularis* [$Q_m = 0.735 -$
 279 $0.133 \cdot \text{depth}$; $R^2=0.71$, $p<0.001$] and *O. franksi* [$Q_m = 0.422 - 0.054 \cdot \text{depth}$; $R^2=0.50$, $p<0.001$]. Clear lines
 280 represent 95% confidence intervals.

281

282 **Changes in depth produces a major shift in *O. annularis* microbiome**

283 After quality control, sequencing resulted in a total of 577,930 microbial reads (per sample median:
 284 5,758; per sample mean: 9,173) partitioned across 14,274 unique OTUs. Overall, coral-associated
 285 prokaryote communities were significantly structured according to depth ($p = 0.001$), but not host

286 species ($p = 0.12$) or depth by species interaction ($p = 0.86$; PERMANOVA on weighted UniFrac; **Fig. 3**).
 287 The change across depths is mainly driven by *O. annularis* ($p = 0.01$, **Fig. 3**). The strong response of *O.*
 288 *annularis* microbiomes to changes in depth can be visualized in differential patterns of OTU abundance
 289 among depths (**Fig. 3a**).



290

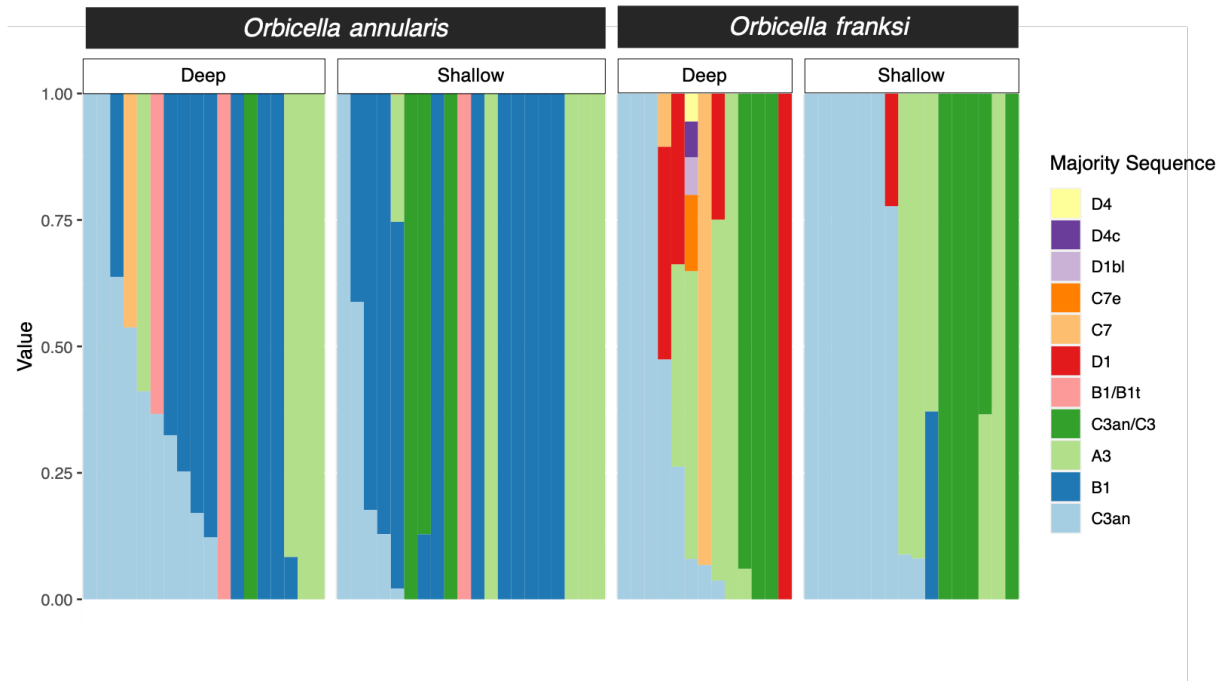
291 **Figure 3.** *O. annularis* microbiomes vary across timepoints and depths while *O. franksi* communities
 292 remain consistent. (a) Relative abundances of the 250 most common OTUs reveal distinct patterns
 293 among *O. annularis* microbiomes at the two transplant depths while *O. franksi* abundance patterns
 294 remain largely consistent across treatments. Each column in the heatmap represents an individual
 295 microbiome sample and phylogenetic relationships among OTUs are shown on the left (FastTree
 296 maximum-likelihood tree). (b) Microbiome variability (*i.e.*, weighted UniFrac distances) was greatest in
 297 *O. annularis* corals transplanted to deep waters. Microbiome variability was higher in corals in deep
 298 waters than in shallow.
 299

300 Ten bacterial taxa were significantly enriched in shallow-water samples. OTUs enriched in shallow-water
301 coral microbiomes are from the bacterial Orders Acidimicrobiales (1 OTU), Alteromonadales (1),
302 Kiloniellales (2), Lactobacillales (1), Neisseriales (1), Oceanospirillales (3), and Synechococcales (1). The
303 mean \log_2 fold change for enriched OTUs was 5.6.

304 Microbiome variability did not differ significantly between species with *O. annularis* (0.592 ± 0.008 ;
305 mean UniFrac distance \pm standard error) and *O. franksi* fragments (0.582 ± 0.008) ($p_{\text{adj}} = 0.358$). In
306 contrast, microbiome variability differed significantly between depths, being greatest in *O. annularis*
307 transplanted S-D (0.631 ± 0.013 ; mean UniFrac distance \pm standard error) and significantly higher than
308 *O. annularis* transplanted S-S (0.574 ± 0.008 ; $p_{\text{adj}} < 0.001$) or *O. franksi* transplanted D-S (0.580 ± 0.010 ;
309 $p_{\text{adj}} = 0.006$) (**Fig. 3b**). The larger microbiome variability in *O. annularis* transplanted deep is consistent
310 with higher mortality and limited photoacclimation potential.

311 ***Symbiodiniaceae communities vary across species***

312 Algal communities of *O. annularis* were significantly different from those of *O. franksi* regardless of the
313 depth to which they were transplanted to ($p < 0.05$; pairwise PERMANOVA on a Bray-Curtis matrix).
314 Symbiodiniaceae genotypes belonging to the genus *Symbiodinium* (ITS2 type A3) and *Cladocopium*
315 (C3an, C3an/C3, C7, and C7f) occurred in both coral species, although *Cladocopium* genotypes were
316 more abundant in *O. franksi*. Genotypes from the genus *Breviolum* (B1 and B1/B1t) were detected in
317 high abundances in *O. annularis*, and in many colonies from the shallow site (40% of them) were the
318 only dominant symbiont. Only one *O. franksi* colony transplanted D-S hosted a *Breviolum* (B1)
319 population. Genotypes belonging to the genus *Durusdinium* (D1, D1bl, D4, and D4c) were detected only
320 in *O. franksi* transplanted D-D (**Fig. 4**). Neither *O. annularis* nor *O. franksi* Symbiodiniaceae communities
321 were significantly different when transplanted to a different depth ($p > 0.1$; pairwise PERMANOVA on a
322 Bray-Curtis matrix).



323
324 **Figure 4.** Relative abundance bar plot of Symbiodiniaceae ITS2 profiles identified in *Orbicella* spp. by
325 Symportal (Hume et al. 2019). Variation in Symbiodiniaceae types is shown by species as well as by
326 depth.
327

328 DISCUSSION

329 Our study demonstrates that despite being genetically close (Levitan et al. 2011), *O. annularis* and *O.*
330 *franksi* have diverged physiologically and occupy distinct light environments in part due to the variation
331 in their associated microbiotas (Symbiodiniaceae and bacterial communities). Following transplantation
332 to deep habitats, *O. annularis* experiences a limited photoacclimation potential and disruption of the
333 photosynthetic performance of its algal symbionts, consistent with increased mortality and significant
334 microbiome community shifts with increased variability. By contrast, *O. franksi* maintained a robust
335 physiological performance, a resilient microbiome composition with no significant community shifts or
336 increased variability, and low mortality at both depths. Our study suggests that *O. annularis* is adapted
337 to shallow environments characterized by a higher and more variable temperature and light regimes,
338 while *O. franksi* is physiologically able to live in both shallow and deep habitats. The niches of these
339 sibling species have diverged, and a large component of the niche separation seems to be related to
340 variations in the photoacclimation capabilities and the microbial community of each species. The
341 absence of *O. franksi* in shallow areas may be related to other ecological aspects such as slow growth in

342 an area of intense space competition, a restricted morphological plasticity for regulating the light
343 capture (see below) and/or non-random settlement of recruits across depths (*i.e.*, larval habitat choice).

344 ***The vertical distribution couples with the photoacclimation capabilities of each species***

345 The vertical distribution of *O. annularis* and *O. franksi* is compressed toward shallower depths in Bocas
346 del Toro compared to other clear-water sites in the Caribbean (*e.g.*, Curaçao (Van Veghel 1994) and
347 Belize (Pandolfi and Budd 2008)). The vertical habitat compression in both species is consistent with the
348 K_d measured in Bocas del Toro (0.40 m^{-1}), which is notably higher than in clear-water sites (0.06 m^{-1} in
349 Curaçao and 0.08 m^{-1} in Belize (Banaszak et al. 1998; Vermeij and Bak 2002)) and reflects the effect of
350 the heavy rainfall patterns and runoff in the region on the optical properties of the water column
351 (Kaufmann and Thompson 2005). This vertical habitat compression is consistent with other coral reefs
352 exposed to water turbidity (Morgan et al. 2020; López-Londoño et al. 2021) and suggest that the light
353 penetration into the water column associated with the local K_d is a determinant factor for the vertical
354 zonation of *Orbicella* spp. Despite local differences in the vertical distribution ranges, *O. annularis*
355 consistently occupies well-lit shallow areas of reefs where the potential for increased photosynthesis
356 and calcification rates drives a steep competition for space with other corals. In contrast, *O. franksi*
357 consistently dominates deeper reef areas characterized by low-light conditions and reduced coral-
358 growth rates (Cohen and Dubinsky 2015).

359 Our findings indicate that *O. annularis* experiences an almost complete loss of photosynthetic activity
360 when transplanted deep. *O. annularis* fragments photoacclimate to low-light conditions by increasing
361 the light energy conversion efficiency (*i.e.*, increase in F_v/F_m) (Hoegh-Guldberg and Jones 1999; Gorbunov
362 et al. 2001). However, the extremely low values of Q_m reflect a trivial photosynthetic contribution of *O.*
363 *annularis* symbionts to the host metabolism due to light-limited photosynthesis (Iglesias-Prieto et al.
364 2004), suggesting that the photoacclimation potential is insufficient to compensate for the low-light
365 conditions of deep environments. Photoacclimation of *O. franksi* fragments transplanted to the shallow
366 environment resulted in an increased fraction of photo-inactivated PSII reaction centers and capacity for
367 thermal dissipation of excessive light energy absorbed (Hoegh-Guldberg and Jones 1999; Gorbunov et al.
368 2001). But in contrast to *O. annularis*, the estimated Q_m in *O. franksi* do not indicate the occurrence of
369 chronic photoinhibition in the shallow environment nor light-limitation in the deep environment,
370 suggesting that *O. franksi* can maintain a more robust physiological performance across depths. The
371 photoacclimation responses of both species in the transplant experiment were consistent with the rates

372 of change in Q_m across their vertical distribution range, which collectively suggest that the symbiotic
373 algae of *O. annularis* are more sensitive to changes in light intensity with depth than symbionts of *O.*
374 *franksi*.

375 Colony morphology can help modulate the light capture and photosynthetic energy acquisition along
376 the vertical distribution range of corals (Hoogenboom et al. 2008; Kaniewska et al. 2011). The
377 dominance of *O. annularis* in shallow habitats correlates with its faster vertical growth among *Orbicella*
378 species (Weil and Knowlton 1994). Its morphology (typically columnar) helps regulate the distribution of
379 light energy for symbiotic algae across the colony surface, representing an advantageous strategy in
380 high-light environments because it reduces the coral tissue area subjected to excessive irradiance
381 (Kaniewska et al. 2011). When transplanted deep, this morphology may lead to acute light energy
382 limitation which, in combination with the insufficient acclimation potential to compensate for low-light,
383 can lead to negative energetic balances for the whole colony and eventual death. *O. franksi*, on the
384 other hand, produce plate-like colonies to maximize light capture in deep environments. When
385 transplanted to shallow well-lit environments, despite a potential for successful photoacclimation as
386 indicated by our results, the plate-like morphology limits the capacity to regulate the internal light
387 climate and allows very slow vertical growth. This slow growth makes *O. franksi* a poor competitor, likely
388 explaining why this species is rare in shallow areas. Alternatively, and not mutually exclusive, their larvae
389 may preferentially settle in low light environments. In fact, adaptation and strong selection across
390 depths, may promote the evolution of habitat choice.

391 ***Host species drive symbiont communities***

392 Species-specific associations with algal symbionts with contrasting photoacclimation capabilities may be
393 a key axis of differentiation between *O. annularis* and *O. franksi*. Despite the higher and more variable
394 temperature and light intensity in shallow areas, which are known conditions that promote the
395 association with *Durusdinium trenchii* in other corals (Lajeunesse et al. 2009), this dinoflagellate was not
396 detected in *O. annularis* colonies. Surprisingly, this thermotolerant symbiont (ITS type D1/D1bl) was
397 found in nearly 20% of *O. franksi* colonies from the deep environment. The increased abundance of *D.*
398 *trenchii* in *O. franksi* may be related with the runoff impacts in the water column (*e.g.*, sedimentation
399 and nutrient enrichment), a reduction in light penetration, and the mechanisms by which the coral-algae
400 symbiosis interact with these environmental conditions (Garren et al. 2006). The prevalence of
401 *Breviolum* genotypes in *O. annularis* and *Cladocopium* genotypes in *O. franksi*, both in the shallow and

402 deep transplant sites, is consistent with previous reports (LaJeunesse 2002; Garren et al. 2006) and may
403 indicate the formation of stable associations explained by the photoacclimative capabilities of
404 dinoflagellates and the variability of physical factors within the vertical distribution range of each coral
405 species (LaJeunesse 2002; Iglesias-Prieto et al. 2004). The ITS2 analysis has a low resolution to
406 differentiate lineages within the same genus in symbiotic algal communities (LaJeunesse and Thornhill
407 2011; Stat et al. 2011). It is possible that complementary analysis with other molecular markers
408 improves the phylogenetic resolution of Symbiodiniaceae (*i.e.*, species or population level), detecting
409 differences in cryptic species/populations of *Cladocopium* spp. or *Breviolum* spp. uniquely associated
410 with each *Orbicella* species like in other depth-segregated anthozoans (Prada et al. 2014; Pochon et al.
411 2015).

412 ***Microbiome communities vary across depths and are enriched in shallow habitats***

413 Several Endozoicomonas OTUs were significantly enriched in shallow habitats. Endozoicomonaceae are
414 diverse gammaproteobacterial symbionts of numerous marine hosts at varying depths and with a wide
415 global distribution (Neave et al. 2016). Members of this group are found in abundance in the tissues of
416 coral species and are considered to be true symbionts of corals which may provide a beneficial function
417 (Bayer et al. 2013; Pantos et al. 2015). Although their function within the coral host is not entirely clear;
418 proposed benefits include nutrient acquisition, microbiome structuring and roles in coral health.

419 Members of the family Alteromonadaceae and the order Acidimicrobiales were also enriched in shallow
420 areas. Alteromonadaceae belong to a diverse group of heterotrophic gammaproteobacteria known to
421 associate with marine hosts and nutrient rich environments. Members of this group tolerate relatively
422 high temperatures and have been used in coral probiotic studies as coral-associated bacteria capable of
423 scavenging free radicals (Dungan et al. 2020), and therefore could provide similar benefits in shallow,
424 high-light environments. Similarly, Acidimicrobiales are known to be planktonic free-living photo-
425 heterotrophs found in both temperal and tropical photic zones (Angly et al. 2016) and are associated
426 with DOM in marine environments (Osterholz et al. 2018).

427 Finally, corals in shallow areas were also enriched for *Alloiococcus* and *Synechococcus*. *Alloiococcus*
428 belongs to the group of gram-positive lactic acid bacteria, which are recognized for producing bacterial
429 growth inhibitors that function to deter invading bacteria in their hosts (Ringø et al. 2018).

430 *Synechococcus* is a photoautotrophic cyanobacterium found in surface waters harbouring abundant
431 light. Both corals and their symbiotic algae are known to actively feed on *Synechococcus* (Jeong et al.

432 2012; McNally et al. 2017) which is often found as a member of the coral surface mucus microbiome
433 (Marchioro et al. 2020). As a food for corals, it has been suggested that nitrogen-rich *Synechococcus*
434 cells may increase bleaching recovery and coral health (Meunier et al. 2019).

435 There is a continuing debate as to the relative role of coral host vs. environment in shaping coral
436 microbiomes. This study demonstrates that the responsiveness of coral microbiomes to environmental
437 conditions differs significantly even among very closely related coral species. These differences in
438 microbiome shifts may be related to the resilience of the coral host and its associated algal community
439 to a particular habitat. Pantos et al. (Pantos et al. 2015) found that environment is the major driver of
440 microbiome structure in *Seriatopora hystrix*, not host genotype or Symbiodiniaceae strain. Our results
441 do not contradict this finding but suggest that responsiveness to environmental conditions can differ
442 significantly even among very closely related coral taxa.

443 ***Implications for coral reef conservation***

444 A key finding in our study with implications for coral restoration is the increased mortality of *O.*
445 *annularis* when transplanted to low-light environments. We suggest that to enhance survivorship during
446 restoration, the particular light environment of source populations should be similar to the transplant
447 sites. In this study, due to the high vertical attenuation of light ($K_d = 0.40 \text{ m}^{-1}$), a 6 m increase in depth
448 resulted in an order of magnitude reduction in irradiance and increased mortality of *O. annularis* by
449 26%. In a clear-water site (*e.g.*, $K_d = 0.06 \text{ m}^{-1}$), this response would be expected to occur with an increase
450 in depth of ~ 40 m. Giving the expensive nature of coral restoration, equating the light environment of
451 donor and transplant sites will likely increase yield and decrease costs. Minimally, our approach can be
452 used to estimate the maximum theoretical depth for each species in a given location with certain water
453 optical quality, thereby providing guidance when choosing the location and depth for coral
454 transplantation.

455 The second aspect of our findings is related to microbiome composition in different habitats across
456 reefs. Shallow water reefs are areas of high stress with strong variations in light, temperature and
457 salinity, strong changes in water motion and sediment transport, and more ecological variability. Our
458 study suggests that the microbiome of shallow water specialists like *O. annularis* is fine-tuned to this
459 environment and a reduction in the light field can cascade into drastic changes to host-associated
460 microbial community composition. Increases in temperature as a result of climate change has affected
461 primarily shallow water corals (Bridge et al. 2013; Hughes et al. 2018), suggesting that instability in the

462 coral microbiomes of shallow-water corals will increase, likely accelerating coral decline of these reef
463 areas.

464 Lastly, subtle differences in the water optical conditions can result in changes in the underwater light
465 environment and the vertical distribution of coral species. Most coral reefs around the globe are
466 currently threatened by the direct effects of sediments, pollutants and nutrients associated with coastal
467 development and terrestrial runoff (Carlson et al. 2019). These conditions affect the water optical
468 quality and, as a consequence, the light climate of corals and the survivorship of species at different
469 depths. Although previous studies have suggested that deep-water species are more sensitive to
470 changes in water optical conditions (Vermeij and Bak 2002), our results suggest that at least some
471 shallow-water specialists, like *O. annularis*, can be extremely vulnerable to these changes as their
472 physiology/morphology is specialized for high light habitats. As the degradation of water optical
473 properties in coral reefs continue, shallow-water specialists, which are typically major reef-building
474 species, will likely become rare, shifting the structural and functional integrity of reefs.

475 CONCLUSION

476 Our study suggests that the sibling coral species, *O. annularis* and *O. franksi*, are adapted to distinctive
477 light environments along depth gradients. The limited photoacclimation potential and less robust
478 microbiome community restricts *O. annularis* to shallow, high-light environments. *O. franksi* is more
479 versatile, but other ecological aspects such as slow growth in areas of intense space competition
480 restricts the species to deep environments. These contrasting responses associated with the microbial
481 communities highlight the importance of niche specialization in symbiotic corals for the maintenance of
482 species diversity. Our study has implications on coral reef restoration efforts, providing guidance when
483 choosing the location, depth and light environment for coral transplantation.

484 ACKNOWLEDGMENTS

485 Arcadio Castillo Díaz, Gabriel Jácome and Plinio Góndola from the Smithsonian Tropical Research
486 Institute assisted with field operations at the Bocas del Toro field station. Gaby Swain helped on sample
487 processing. Dr. Benjamin Hume provided assistance on Symbiodiniaceae analysis through the SymPortal
488 framework.

489 FUNDING STATEMENT

490 This work was supported by NSF grants OCE 1442206 and OCE 1642311; Pennsylvania State University
491 startup funds to MM and RI-P; and NOAA grant NA19NOS4820132. CP was funded by grants from NSF
492 (OIA) 2032919 and USDA National Institute of Food and Agriculture (Hatch) 1017848.

493 COMPETING INTERESTS

494 The authors declare that they have no competing interests.

495 REFERENCES

- 496 Angly FE, Heath C, Morgan TC, Tonin H, Rich V, Schaffelke B, Bourne DG, Tyson GW (2016) Marine microbial
497 communities of the Great Barrier Reef lagoon are influenced by riverine floodwaters and seasonal
498 weather events. *PeerJ* 4:e1511
- 499 Apprill A, McNally S, Parsons R, Webe L (2015) Minor revision to V4 region SSU rRNA 806R gene primer greatly
500 increases detection of SAR11 bacterioplankton. *Aquat Microb Ecol* 75:129–137
- 501 Banaszak A, Lesser M, Kuffner I, Ondrusek M (1998) Relationship between ultraviolet (UV) radiation and
502 mycosporine-like amino acids (MAAS) in marine organisms. *Bull Mar Sci* 63:617-628
- 503 Bayer T, Neave MJ, Alsheikh-Hussain A, Aranda M, Yum LK, Mincer T, Hughen K, Apprill A, Voolstra CR (2013) The
504 microbiome of the Red Sea coral *Stylophora pistillata* is dominated by tissue-associated Endozoicomonas
505 bacteria. *Appl Environ Microbiol* 79:4759-4762
- 506 Bridge TC, Hoey AS, Campbell SJ, Muttaqin E, Rudi E, Fadli N, Baird AH (2013) Depth-dependent mortality of reef
507 corals following a severe bleaching event: implications for thermal refuges and population recovery.
508 *F1000Research* 2
- 509 Caporaso JG, Bittinger K, Bushman FD, DeSantis TZ, Andersen GL, Knight R (2010a) PyNAST: a flexible tool for
510 aligning sequences to a template alignment. *Bioinformatics* 26:266-267
- 511 Caporaso JG, Kuczynski J, Stombaugh J, Bittinger K, Bushman FD, Costello EK, Fierer N, Pena AG, Goodrich JK,
512 Gordon JI (2010b) QIIME allows analysis of high-throughput community sequencing data. *Nat Methods*
513 7:335-336
- 514 Carlson RR, Foo SA, Asner GP (2019) Land use impacts on coral reef health: a ridge-to-reef perspective. *Front Mar*
515 *Sci* 6:562
- 516 Cohen I, Dubinsky Z (2015) Long term photoacclimation responses of the coral *Stylophora pistillata* to reciprocal
517 deep to shallow transplantation: Photosynthesis and calcification. *Front Mar Sci* 2
- 518 Dungan AM, Bulach D, Lin H, van Oppen MJH, Blackall LL (2020) Development of a free radical scavenging probiotic
519 to mitigate coral bleaching. *bioRxiv:2020.2007.2002.185645*
- 520 Edgar RC (2010) Search and clustering orders of magnitude faster than BLAST. *Bioinformatics* 26:2460-2461
- 521 Fukami H, Budd AF, Levitan DR, Jara J, Kersanach R, Knowlton N (2004) Geographical differences in species
522 boundaries among members of the *Montastraea annularis* complex based on molecular and
523 morphological markers. *Evolution* 58:324-337
- 524 Garren M, Walsh SM, Caccone A, Knowlton N (2006) Patterns of association between Symbiodinium and members
525 of the *Montastraea annularis* species complex on spatial scales ranging from within colonies to between
526 geographic regions. *Coral Reefs* 25:503-512
- 527 Gilbert SF, McDonald E, Boyle N, Buttino N, Gyi L, Mai M, Prakash N, Robinson J (2010) Symbiosis as a source of
528 selectable epigenetic variation: taking the heat for the big guy. *Phil Trans R Soc B* 365:671-678
- 529 Gorbunov MY, Kolber ZS, Lesser MP, Falkowski PG (2001) Photosynthesis and photoprotection in symbiotic corals.
530 *Limnol Oceanogr* 46:75-85
- 531 Hereford J (2009) A quantitative survey of local adaptation and fitness trade-offs. *Am Nat* 173:579-588

- 532 Hoegh-Guldberg O, Jones RJ (1999) Photoinhibition and photoprotection in symbiotic dinoflagellates from reef-
533 building corals. *Mar Ecol Prog Ser* 183:73-86
- 534 Hoogenboom MO, Connolly SR, Anthony KRN (2008) Interactions between morphological and physiological
535 plasticity optimize energy acquisition in corals. *Ecology* 89:1144-1154
- 536 Hughes TP, Kerry JT, Baird AH, Connolly SR, Dietzel A, Eakin CM, Heron SF, Hoey AS, Hoogenboom MO, Liu G,
537 McWilliam MJ, Pears RJ, Pratchett MS, Skirving WJ, Stella JS, Torda G (2018) Global warming transforms
538 coral reef assemblages. *Nature* 556:492-496
- 539 Hume BCC, Smith EG, Ziegler M, Warrington HJM, Burt JA, LaJeunesse TC, Wiedenmann J, Voolstra CR (2019)
540 SymPortal: a novel analytical framework and platform for coral algal symbiont next-generation
541 sequencing ITS2 profiling. *Mol Ecol Resour* 19:1063-1080
- 542 Iglesias-Prieto R, Beltran VH, LaJeunesse TC, Reyes-Bonilla H, Thome PE (2004) Different algal symbionts explain
543 the vertical distribution of dominant reef corals in the eastern Pacific. *Proc R Soc Lond B* 271:1757-1763
- 544 Jeong HJ, Du Yoo Y, Kang NS, Lim AS, Seong KA, Lee SY, Lee MJ, Lee KH, Kim HS, Shin W (2012) Heterotrophic
545 feeding as a newly identified survival strategy of the dinoflagellate *Symbiodinium*. *Proc Natl Acad Sci USA*
546 109:12604-12609
- 547 Kaniewska P, Magnusson SH, Anthony KRN, Reef R, Kühl M, Hoegh-Guldberg O (2011) Importance of macro- versus
548 microstructure in modulating light levels inside coral colonies. *J Phycol* 47:846-860
- 549 Kaufmann KW, Thompson RC (2005) Water temperature variation and the meteorological and hydrographic
550 environment of Bocas del Toro, Panama. *Caribb J Sci* 41:392-413
- 551 Kellogg CA, Piceno YM, Tom LM, DeSantis TZ, Gray MA, Zawada DG, Andersen GL (2013) Comparing bacterial
552 community composition between healthy and white plague-like disease states in *Orbicella annularis* using
553 PhyloChip™ G3 microarrays. *PLoS ONE* 8:e79801
- 554 Kemp DW, Thornhill DJ, Rotjan RD, Iglesias-Prieto R, Fitt WK, Schmidt GW (2015) Spatially distinct and regionally
555 endemic *Symbiodinium* assemblages in the threatened Caribbean reef-building coral *Orbicella faveolata*.
556 *Coral Reefs* 34:535-547
- 557 Kirk JTO (2011) *Light and photosynthesis in aquatic ecosystems*. Cambridge University Press, New York
- 558 Lahti L, Shetty S (2017) microbiome R package. Tools for microbiome analysis in R.
- 559 LaJeunesse T (2002) Diversity and community structure of symbiotic dinoflagellates from Caribbean coral reefs.
560 *Mar Biol* 141:387-400
- 561 LaJeunesse TC, Thornhill DJ (2011) Improved resolution of reef-coral endosymbiont (*Symbiodinium*) species
562 diversity, ecology, and evolution through psbA non-coding region genotyping. *PLoS ONE* 6:e29013
- 563 LaJeunesse TC, Smith RT, Finney J, Oxenford H (2009) Outbreak and persistence of opportunistic symbiotic
564 dinoflagellates during the 2005 Caribbean mass coral bleaching event. *Proc R Soc B* 276:4139-4148
- 565 Levitan D, Fogarty N, Jara J, Lotterhos K, Knowlton N (2011) Genetic, spatial, and temporal components to precise
566 spawning synchrony in reef building corals of the *Montastraea annularis* species complex. *Evolution*
567 65:1254-1270
- 568 López-Londoño T, Galindo-Martínez CT, Gómez-Campo K, González-Guerrero LA, Roitman S, Pollock FJ, Pizarro V,
569 López-Victoria M, Medina M, Iglesias-Prieto R (2021) Physiological and ecological consequences of the
570 water optical properties degradation on reef corals. *Coral Reefs* 40:1243-1256
- 571 Love MI, Huber W, Anders S (2014) Moderated estimation of fold change and dispersion for RNA-seq data with
572 DESeq2. *Genome Biol* 15:550
- 573 Marchioro GM, Glasl B, Engelen AH, Serrão EA, Bourne DG, Webster NS, Frade PR (2020) Microbiome dynamics in
574 the tissue and mucus of acroporid corals differ in relation to host and environmental parameters. *PeerJ*
575 8:e9644
- 576 McDonald D, Price MN, Goodrich J, Nawrocki EP, DeSantis TZ, Probst A, Andersen GL, Knight R, Hugenholtz P
577 (2012) An improved Greengenes taxonomy with explicit ranks for ecological and evolutionary analyses of
578 bacteria and archaea. *ISME J* 6:610-618
- 579 McMurdie PJ, Holmes S (2013) phyloseq: an R package for reproducible interactive analysis and graphics of
580 microbiome census data. *PLoS ONE* 8:e61217
- 581 McNally SP, Parsons RJ, Santoro AE, Apprill A (2017) Multifaceted impacts of the stony coral *Porites astreoides* on
582 picoplankton abundance and community composition. *Limnol Oceanogr* 62:217-234
- 583 Meunier V, Bonnet S, Pernice M, Benavides M, Lorrain A, Grosso O, Lambert C, Houlbrèque F (2019) Bleaching
584 forces coral's heterotrophy on diazotrophs and *Synechococcus*. *ISME J* 13:2882-2886

- 585 Morgan KM, Moynihan MA, Sanwlani N, Switzer AD (2020) Light Limitation and Depth-Variable Sedimentation
586 Drives Vertical Reef Compression on Turbid Coral Reefs. *Frontiers in Marine Science* 7:931
- 587 Neave MJ, Apprill A, Ferrier-Pagès C, Voolstra CR (2016) Diversity and function of prevalent symbiotic marine
588 bacteria in the genus *Endozoicomonas*. *Appl Microbiol Biotechnol* 100:8315-8324
- 589 Oksanen J, Blanchet FG, Friendly M, Kindt R, Legendre P, McGlenn D, Minchin PR, O'Hara RB, Simpson GL, Solymos
590 P, Stevens MHH, Szoecs E, Wagner H (2017) *vegan*: Community Ecology Package
- 591 Osterholz H, Kirchman DL, Niggemann J, Dittmar T (2018) Diversity of bacterial communities and dissolved organic
592 matter in a temperate estuary. *FEMS Microbiol Ecol* 94:fiy119
- 593 Pandolfi JM, Budd AF (2008) Morphology and ecological zonation of Caribbean reef corals: the *Montastraea*
594 'annularis' species complex. *Mar Ecol Prog Ser* 369:89-102
- 595 Pandolfi JM, Lovelock CE, Budd AF (2002) Character release following extinction in a Caribbean reef coral species
596 complex. *Evolution* 56:479-501
- 597 Pantos O, Bongaerts P, Dennis PG, Tyson GW, Hoegh-Guldberg O (2015) Habitat-specific environmental conditions
598 primarily control the microbiomes of the coral *Seriatopora hystrix*. *ISME J* 9:1916-1927
- 599 Peixoto RS, Rosado PM, Leite DCdA, Rosado AS, Bourne DG (2017) Beneficial microorganisms for corals (BMC):
600 proposed mechanisms for coral health and resilience. *Front Microbiol* 8:341
- 601 Pochon X, Forsman ZH, Spalding HL, Padilla-Gamiño JL, Smith CM, Gates RD (2015) Depth specialization in
602 mesophotic corals (*Leptoseris* spp.) and associated algal symbionts in Hawai'i. *R Soc Open Sci* 2:140351
- 603 Prada C, McIlroy SE, Beltrán DM, Valint DJ, Ford SA, Hellberg ME, Coffroth MA (2014) Cryptic diversity hides host
604 and habitat specialization in a gorgonian-algal symbiosis. *Mol Ecol* 23:3330-3340
- 605 Price MN, Dehal PS, Arkin AP (2010) FastTree 2—approximately maximum-likelihood trees for large alignments.
606 *PLoS ONE* 5:e9490
- 607 R Core Team (2015) *R: A language and environment for statistical computing* R Foundation for Statistical
608 Computing. R Foundation for Statistical Computing, Vienna, Austria
- 609 Ralph P, Gademann R (2005) Rapid Light Curves: a powerful tool to assess photosynthetic activity. *Aquat Bot*
610 82:222-237
- 611 Rideout JR, He Y, Navas-Molina JA, Walters WA, Ursell LK, Gibbons SM, Chase J, McDonald D, Gonzalez A, Robbins-
612 Pianka A, others (2014) Subsampled open-reference clustering creates consistent, comprehensive OTU
613 definitions and scales to billions of sequences. *PeerJ* 2:e545
- 614 Ringø E, Hoseinifar SH, Ghosh K, Doan HV, Beck BR, Song SK (2018) Lactic acid bacteria in finfish—An update. *Front*
615 *microbiol* 9:1818
- 616 Rohwer F, Seguritan V, Azam F, Knowlton N (2002) Diversity and distribution of coral-associated bacteria. *Mar Ecol*
617 *Prog Ser* 243:1-10
- 618 Roitman S, López-Londoño T, Joseph Pollock F, Ritchie KB, Galindo-Martínez CT, Gómez-Campo K, González-
619 Guerrero LA, Pizarro V, López-Victoria M, Iglesias-Prieto R, Medina M (2020) Surviving marginalized reefs:
620 assessing the implications of the microbiome on coral physiology and survivorship. *Coral Reefs* 39:795-
621 807
- 622 Rowan R, Knowlton N, Baker A, Jara J (1997) Landscape ecology of algal symbionts creates variation in episodes of
623 coral bleaching. *Nature* 388:265-269
- 624 Scheufen T, Kramer WE, Iglesias-Prieto R, Enriquez S (2017) Seasonal variation modulates coral sensibility to heat-
625 stress and explains annual changes in coral productivity. *Sci Rep* 7:4937
- 626 Schloss PD, Westcott SL, Ryabin T, Hall JR, Hartmann M, Hollister EB, Lesniewski RA, Oakley BB, Parks DH, Robinson
627 CJ, Sahl JW, Stres B, Thallinger GG, Van Horn DJ, Weber CF (2009) Introducing mothur: open-source,
628 platform-independent, community-supported software for describing and comparing microbial
629 communities. *Appl Environ Microbiol* 75:7537-7541
- 630 Stat M, Pochon X, Cowie ROM, Gates RD (2009) Specificity in communities of Symbiodinium in corals from
631 Johnston Atoll. *Mar Ecol Prog Ser* 386:83-96
- 632 Stat M, Bird CE, Pochon X, Chasqui L, Chauka LJ, Concepcion GT, Logan D, Takabayashi M, Toonen RJ, Gates RD
633 (2011) Variation in Symbiodinium ITS2 sequence assemblages among coral colonies. *PLoS ONE* 6:e15854
- 634 Stoddart DR (1969) Ecology and morphology of recent coral reefs. *Biol Rev* 44:433-498
- 635 Thompson JR, Rivera HE, Closek CJ, Medina M (2015) Microbes in the coral holobiont: partners through evolution,
636 development, and ecological interactions. *Front Cell Infect Microbiol* 4:1-20

- 637 Van Veghel MLJ (1994) Polymorphism in the Caribbean reef building coral *Montastrea annularis*. Ph.D. thesis.
638 University of Amsterdam, p128
- 639 Vermeij MJA, Bak RPM (2002) How are coral populations structured by light? Marine light regimes and the
640 distribution of *Madracis*. *Mar Ecol Prog Ser* 233:105-116
- 641 Warner ME, LaJeunesse TC, Robison JD, Thur RM (2006) The ecological distribution and comparative photobiology
642 of symbiotic dinoflagellates from reef corals in Belize: potential implications for coral bleaching. *Limnol*
643 *Oceanogr* 51:1887-1897
- 644 Weil E, Knowlton N (1994) A multi-character analysis of the Caribbean coral *Montastraea annularis* (Ellis and
645 Solander, 1786) and its two sibling species, *M. faveolata* (Ellis and Solander, 1786) and *M. franksi*
646 (Gregory, 1895). *Bull Mar Sci* 55:151-175
- 647 Wickham H (2009) *ggplot2: elegant graphics for data analysis*. Springer, New York

648